Relationship Between Thermal Properties, Morphology, and Crystallinity of Nanocomposites Based on Polyhydroxybutyrate

David A. D'Amico, Liliana B. Manfredi, Viviana P. Cyras

INTEMA, Instituto de Investigaciones en Ciencia y Tecnología de Materiales, Facultad de Ingeniería, Universidad Nacional de Mar del Plata, J. B. Justo 4302, Mar del Plata, Argentina

Received 9 April 2010; accepted 3 March 2011
DOI 10.1002/app.34457
Published online 26 July 2011 in Wiley Online Library (wileyonlinelibrary.com).

ABSTRACT: Polyhydroxybutyrate (PHB) has a significant instability at temperature close to the melting point. The aim of this work was to improve the thermal resistance of PHB by the addition of small amounts of two different types of clays: Cloisite® Na^+ (CNa^+) and Cloisite® 15A (C15A). C15A has more hydrophobic character and interlayer distance than CNa^+. It was observed that the addition of the organically modified montmorillonite (MMT) increased by more than 15°C the thermal resistance of the PHB while the addition of CNa^+ reduced it. This result was related to the different morphology of the final materials. The maximum in the degradation temperature of the nanocomposites with 4% of clay was in accordance with the maximum in the percentage of crystallinity. However, the interlayer gallery distance of the C15A was higher than the CNa^+ in the PHB matrix, according to the better thermal stability of the C15A due to the higher barrier effect and the lower chain mobility. A slight increase in the Young modulus of the polymer was observed with the addition of C15A, due to the compatibility between the MMT and PHB. The calorimetric and microscopy results showed that clays did not accelerate the formation of PHB spherulites nucleus, but the lamellar velocity was accelerated. © 2011 Wiley Periodicals, Inc. J Appl Polym Sci 123: 200–208, 2012

Key words: polyhydroxybutyrate; biodegradable nanocomposites; thermal degradation; crystallization

INTRODUCTION

In recent years, there has been emphasis on development of novel biodegradable materials with multiple applications, as well as to improve certain properties of existing materials. Polyhydroxyalkanoates (PHA's), of which poly(hydroxybutyrate) (PHB) is the most common, are biodegradable polymers produced by different types of microorganisms from renewable sources such as sugar and molasses as intracellular storage materials. For this reason, the PHB does not contain any residues of catalysts like other synthetic polymers. PHA's are now under intensive investigation because of its inherent property as biodegradable thermoplastic. PHB is fully biodegradable polyester with optical activity, piezoelectricity, and hydrophobicity, and it is a material with a high melting temperature as well as degree of crystallinity. A very interesting property of PHB is its low O_2, CO_2, and H_2O permeability, which is close to that of low-density polyethylene. However, they are still expensive, have a narrow processability window and are quite stiff and brittle. The degree of brittleness depends on the degree of crystallinity, glass transition temperature, and microstructure.[1–4]

Very low resistance to thermal degradation seems to be the most serious problem related to PHB processing, because after reaching melting point its thermal degradation begins very quickly. The main reaction involves chain scission, which results in a rapid decrease in molecular weight and further degradation to crotonic acid at high temperatures.[1,5–8]

Recently, the development of nanocomposites by incorporating nanoscaled fillers into a polymer matrix is believed to become a key technology on advanced composite materials. It is well-known that nanocomposites obtained by the addition of low percentages of clay to polymers exhibited an improvement in the properties such as, thermal and oxidative barrier when they were compared with traditional composites.[6,9–11] The materials that frequently exhibit remarkable improvements of material properties are those in which the individual silicate layers are separated in the polymer matrix. A few percent of clay properly dispersed creates much higher surface area for polymer/filler interaction compared with conventional composites. One of the methods commonly used to disperse the clay layers

Correspondence to: V. P. Cyras (vpcyras@fi.mdp.edu.ar).
Contract grant sponsor: CONICET.
Contract grant sponsor: SECYT; contract grant number: PIP-0014.

TABLE I
Organic Modifier and Interlayer Distance of the Clays

Clay	Organic modifier	Concentration of modifier	Interlayer distance (d_{001})
Cloisite®Na^+ (CNa)	–	–	11.7 Å
Cloisite®15A (C15A)	$CH3-\underset{\underset{HT}{\vert}}{\overset{\overset{CH3}{\vert}}{N^+}}-HT$	125 meq/100 g clay	31.5 Å

in the polymers is by intercalation from solution. This method is good for the production of thin films by intercalation of polymers with a little or no polarity into the layered structures.[12]

The polymer properties depend on the crystallization conditions, which influence the crystallization kinetics. The clay addition plays a significant role on the morphology and crystallization process. So it is very useful to characterize the crystallization behavior of clay/polymer nanocomposites and relate it with their properties.[7,13]

The aim of this work was to improve the thermal properties of PHB, obtaining nanocomposites with two types of clays with different hydrophobicity. The effect of the clay addition on the morphology and crystallinity was also evaluated and related to the thermal resistance results.

MATERIALS AND METHODS

Materials

A biodegradable polymer, PHB (M_n = 42,500) was kindly supplied by PHB Industrial S. A., Brazil. Montmorillonite Cloisite®Na^+ and organically modified Cloisite®C15A were supplied by Southern Clay Products (TX). The organic modifier and the interlayer distance of the clays are shown in Table I.

Films of PHB and their nanocomposites were obtained by casting process. Different amounts (2, 4, 6, and 10%w/w) of the two kinds of montmorillonites and PHB (used as it was received), were homogeneously dispersed using chloroform as common solvent. A homogeneous solution of PHB in chloroform was prepared by stirring at 450 rpm while heating at 60°C, for 15 min. Then, the solution was placed on glass Petri dishes, and it was allowed to evaporate at room temperature. Nanocomposites were prepared by the addition of a chloroform clay solution, previously sonicated, to the PHB solution. Thereafter, the same procedure to obtain the PHB films was applied. All films were stored in a desiccator at room temperature for 30 days to allow complete crystallization of PHB.[14] The films thickness of PHB and nanocomposites were 0.05 mm.

Methods

X-ray diffraction analyses (XRD) were performed with KCu (λ = 1.54E) radiation in a Philips PW 1710 X-ray diffractometer system. Every scan was recorded in the range of $2\theta = 2 - 36°$ at a scan speed of 2°/min with an X-ray tube operated at 45 kV and 30 mA. The interlayer distance in the structure of montmorillonite Cloisite®Na^+ and Cloisite®C15A was determined.[11]

Thermogravimetric measurements were performed to study the thermal degradation of the films. This test measures the mass loss as a function of temperature or time, for a given program of temperature. The equipment used was a Mettler TA 4000 at a heating rate of 10°C/min under nitrogen atmosphere. The samples (3–7 mg placed in an aluminum pan) were heated up to 500°C.

Differential Scanning Calorimetric (DSC) analysis of nanocomposites was made using a Perkin–Elmer Pyris 1, under nitrogen atmosphere. Samples about 9 mg weight were taken for DSC measurements. The glass transition (T_g), the melting temperatures (T_m) and degree of crystallinity (X_c) of the samples were determined.

The crystallinity was calculated according to the following equation:

$$X_c\ (\%) = \frac{\Delta H_m.(m_C/m_P)}{\Delta H_0}.100 \qquad (1)$$

where ΔH_m was the melting enthalpy measured in the heating or cooling experiments, ΔH_0 is the theoretical enthalpy of PHB 100% crystalline (ΔH_0 = 146 J/g[15]), m_c is the mass of the nanocomposite and m_p is the mass of PHB in the nanocomposite.

Nonisothermal crystallization from the melt was carried out by heating the sample to 200°C and maintaining it for 2 min, and then cooling at 5°C/min to study the melting process. Polarized optical microscopy (POM) was performed on the PHB and nanocomposite films employing a Leica DMLB microscope, with crossed polarizers. A thin sample between two glass cover slips was placed inside the Linkam shearing device and the temperature was

raised at a rate of 20°C/min up to 200°C. The temperature was kept for 2 min to ensure complete melting and therefore, they were cooled at a rate of 50°C/min to the desired crystallization temperature, T_c. The morphological features were captured in a video camera Leica DC 100. The growth of spherulitic diameter as a function of time was monitored.

Test specimens were cut from the films obtained by casting, using the punch to obtain a dog-bone sample following ASTM D882-97. The samples were subjected to microtensile test on an Instron Universal Testing Machine, Model 4467. The crosshead speed was 1 mm/min.

RESULTS AND DISCUSSION

Thermal degradation analysis was performed to evaluate the effect of the addition of clays with different hydrophobicity on the thermal decomposition behavior of PHB. The peak at 260°C in the DTG curves that represents the decomposition of PHB, was shifted to higher temperatures in the nanocomposites with C15A [Fig. 1(a)], indicating that the addition of clay improves the thermal stability of PHB. However, the composites containing CNa^+ showed lesser thermal stability than the pristine polymer [Fig. 1(b)].

The organoclay may have two opposite functions in the thermal stability of nanocomposites: a barrier effect, which should improve the thermal stability or a catalytic effect on the degradation of the polymer matrix, which should decrease their thermal resistance.[16]

In general, the incorporation of clay into the polymer matrix was found to enhance their thermal stability. The clay acts as a heat barrier improving the overall thermal stability of the system. The presence of the filler restricts the polymer chain mobility and assists the char formation, during the thermal decomposition.

Besides, the silicate layers could hold accumulated heat that can act as a heat source to accelerate the decomposition process. In addition, the presence of aluminum Lewis acid sites in the silicate layers would increase the thermal degradation of polyesters by catalyzing the hydrolysis of ester linkages, and then it would produce a diminution of the thermal degradation temperature.[4,6,17,18]

The diminution in the thermal stability of the nanocomposites with the unmodified clay may be explained by considering that the CNa^+ should act as physical barriers obstructing the transport of volatile products out of the nanocomposites during thermal decomposition. In this way, if the crotonic acid (product of degradation of PHB) is not able to escape, it should accelerate the degradation of PHB. Other effect is the catalytic activity of MMT. The Al Lewis acid sites could catalyze the hydrolysis of ester linkages at high temperatures. It has been also

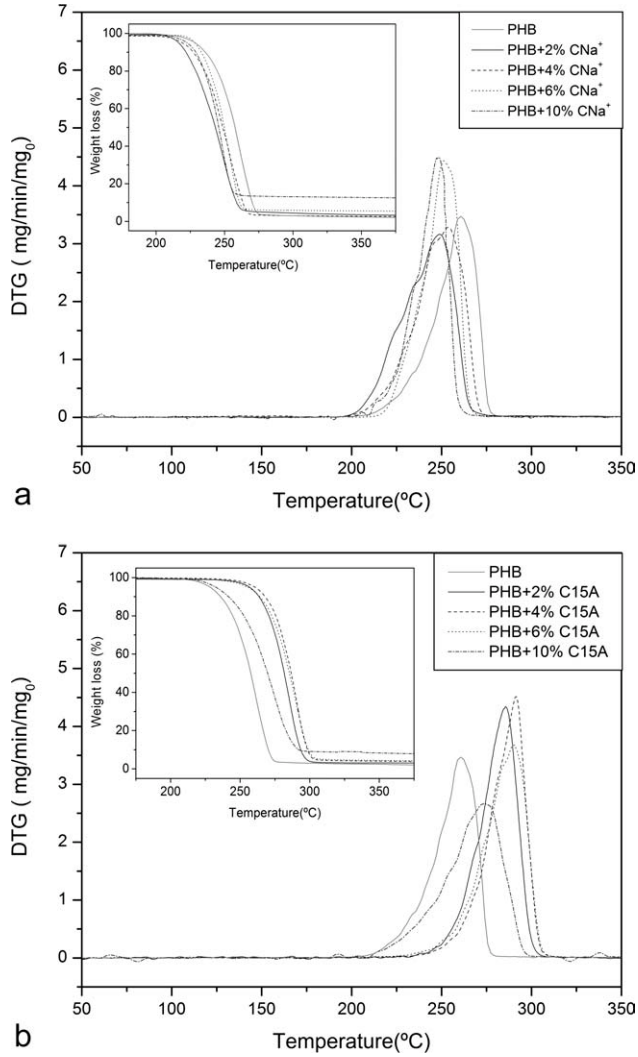

Figure 1 Weight loss and DTG curves for PHB and nanocomposites: (a) PHB/4%CNa^+ and (b) PHB/4%C15A.

argued that after the early stages of thermal decomposition the stacked silicate layers could hold accumulated heat, acting as a heat source to accelerate the decomposition process, in conjunction with the heat flow supplied by the outside heat source.[17,18]

However, the nanocomposites with C15A showed higher degradation temperatures than the PHB. The thermal barrier effect is more important in those composites, and it could be due to the better dispersion of the platelets in the polymer.[11,19] It will be discussed later the relationship among the thermal behavior, clay dispersion, chain mobility, and glass transition temperature.

As shown in Figure 1(a,b), a maximum increase in thermal stability was recorded in the case of the composites containing 4 wt % of clay. An optimum clay loading for thermal stability enhancement was also reported for PS and PET-based nanocomposites.[20] It was suggested that when a low clay fraction is added to the polymer, the thermal barrier

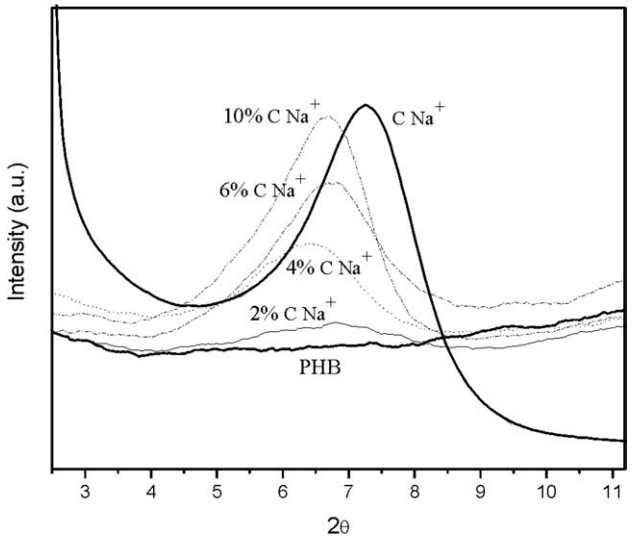

Figure 2 XRD of nanocomposites with Cloisite®Na^+.

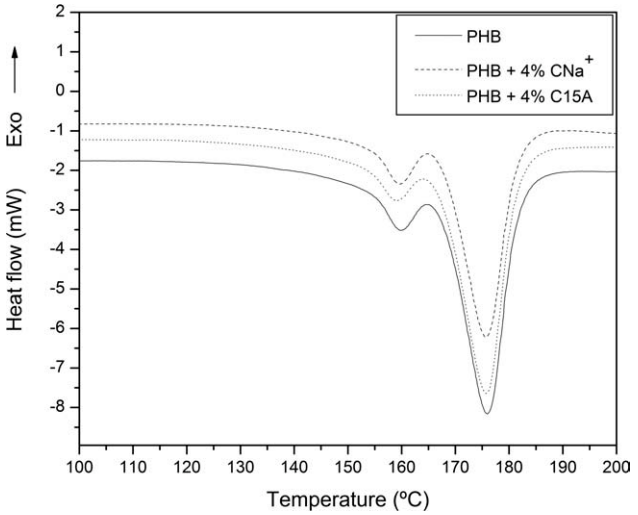

Figure 4 DSC melting curves for PHB, PHB/4%Na^+, and PHB/4% C15A.

effect is predominant because the clay is better dispersed.[21] However, the other effects become dominant with increasing loading, decreasing the thermal stability of the nanocomposite.

To investigate the dispersion of the montmorillonite layers, XRD analyses were performed on the composites. The XRD patterns of the unmodified clay and the composites made with the addition of CNa^+ are showed in Figure 2. It was observed that the MMT exhibits a single 001 diffraction peak around $2\theta = 7.5°$ corresponding to an interlayer distance of 12.2 Å. This basal peak of the MMT was shifted to lower angles in the composite with CNa^+, regardless the clay content. These results should indicate that the clay intergallery region was expanded. The polymer chains entered into the silicate layers forming intercalated PHB/MMT nanocomposites, without reaching complete exfoliation. Inversely, the C15A showed a contraction when was incorporated to the PHB (Fig. 3). The modified montmorillonite (MMT) showed an initial interlayer distance of 33.9 Å, which was reduced up to 28.1 Å when the clay was added to the polymer, shifting the basal peak to higher angles. This contraction could be attributed to a rearrangement of alkyl chains of the clay modifier during the preparation of nanocomposites.[22,23] Duquesne,[19] found a decrease in clay interlayer spacing of Cloisite 30B and Cloisite Na^+ after blending with ethylene vinyl acetate. In spite of this, XRD measurements revealed that the C15A was better dispersed in the polymeric matrix than the CNa^+ because of its higher distance between the clay layers. This result could be related to the higher thermal stability of the nanocomposites containing C15A than PHB and the ones containing CNa^+.

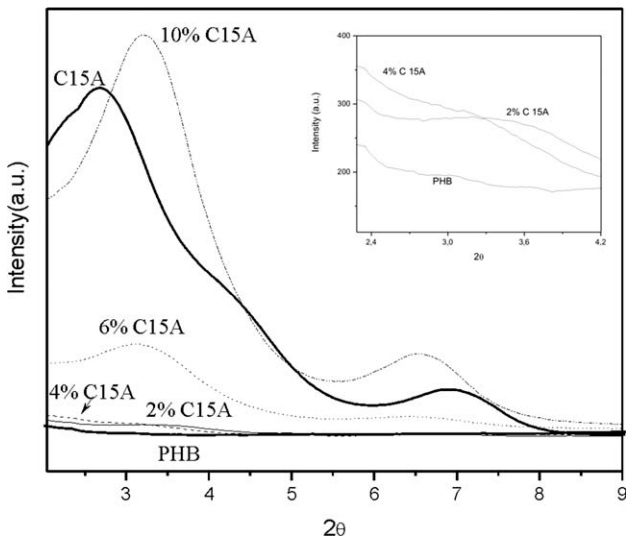

Figure 3 XRD of nanocomposites with Cloisite®C15A.

With the aim to evaluate the influence of the crystallinity on the thermal stability of the nanocomposites, DSC analysis were performed (Fig. 4) and the results were summarized in Table II. In general, it was observed a small diminution in the percentage

TABLE II
Enthalpy of Fusion and Percentage of Crystallinity of the Materials

	T_m (°C)	T_g (°C)	X_c (%)
PHB	175.9	−5.8	66.5
+2% CNa^+	175.8	−4.7	65.1
+4% CNa^+	175.8	−3.7	64.6
+6% CNa^+	176.3	−3.5	63.6
+10% CNa^+	176.2	0.5	63.0
+2% C15A	175.2	−3.6	62.6
+4% C15A	175.7	−2.3	65.9
+6% C15A	175.9	−1.7	62.1
+10% C15A	175.9	1.1	64.3

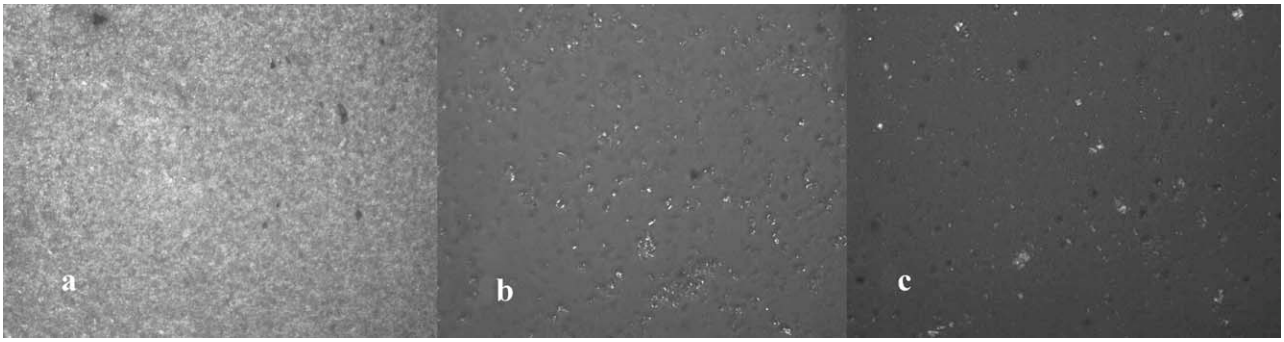

Figure 5 Micrograph obtained by POM (a) PHB/4%CNa^+, (b) melted PHB/4%CNa^+, and (c) suspension of clay CNa^+.

of crystallinity (X_c) of PHB with the addition of clay. The incorporation of the clay had no significant effect on the melting temperatures of the PHB nanocomposites. Likely, the clay are predominantly confined to the amorphous phase, without significantly affecting the development of crystals in the polymer matrix. Nevertheless, the glass transition temperature of the nanocomposites was slightly increased with the addition of the MMTs and it seems to be influenced by the clay dispersion in the polymer. It was observed that the higher was the clay interlayer space, the higher T_g was obtained, comparing the composites PHB/C15A with those PHB/CNa^+. It could be due to the hindrance of segmental motion of the PHB molecular chains by the clay platelets.

The micrographs of the crystalline composites, obtained by POM, revealed that the crystallization morphology was similar between the materials containing CNa^+ and C15A [Figs. 5(a) and 6(a)]. To study the crystalline structure of nanocomposites, the sample containing CNa^+ was melted and the micrograph obtained is shown in Figure 5(b). Birefringence was observed indicating that some crystals, showing an agglomerated arrangement, are still present in the melted sample. They might come from the clay. To confirm this result, a micrograph of an aqueous dispersion of CNa^+ was obtained [Fig. 5(c)] and the clay birefringence was clearly observed too. Similarly, a chloroform dispersion of C15A has also birefringence, as it is showed in Figure 6(c). However, the clay was not observed in the melted C15A nanocomposites [Fig. 6(b)]. These results would indicate that the clay C15A was better dispersed in the PHB with a higher interlayer distance than CNa^+.

The mechanical properties of the nanocomposite films were investigated to characterize the reinforcing effect of the different MMTs and the results are listed in Table III. It was reported that the addition of clay can increase strength as well as modulus, however, the opposite may also occur.[24] It was demonstrated that the addition of C15A only slightly increases the Young's modulus values of the pristine PHB. However, a decrease in the tensile strength of the PHB was also observed in the nanocomposite films. The higher the value of the PHB/C15A modulus, the better the particle intercalation. The collapse of mechanical properties of the nanocomposites containing CNa^+ was attributed to the clay aggregation. A similar behavior was observed for other polymeric systems, including PHA, by several authors.[25,26]

Isothermal crystallization kinetic analysis by spherulitic growth rate (G) was performed by POM, to determine the changes in the crystallization of PHB due to the clay addition. Figure 7 shows optical microscope images (crossed polarizes) corresponding to time evolution of formation of spherulites of PHB,

Figure 6 Micrograph obtained by POM (a) PHB/C15A, (b) melted PHB/4%C15A, and (c) suspension of clay C15A.

TABLE III
Mechanical Properties for the PHB and Nanocomposites

Material	E (GPa)	σ_b (MPa)	ε_b (%)
PHB	4.13 ± 0.15	32.9 ± 2.2	0.91 ± 0.12
PHB + 4% CNa^+	3.09 ± 0.16	24.1 ± 1.5	0.93 ± 0.05
PHB + 4% C15A	4.25 ± 0.27	28.6 ± 4.1	0.74 ± 0.14

PHB/4%CNa^+ and PHB/4%C15A at 90°C. The micrographs revealed that the crystallization morphology was similar among the materials.

The spherulities diameter measured from POM data was plotted versus time (Fig. 8). The slope of that curve was used to calculate the radial growth (G) of PHB spherulities. Thereafter, it was observed that the velocity of crystallization of PHB was enhanced by the presence of the clay, mainly for the C15A, by plotting G versus T_c (Fig. 9**)**.

The radial growth rate of spherulites could be described by the Turnbull and Fisher[27,28] equation:

$$G = G_o \cdot \exp\left(\frac{-E}{R.T}\right) \cdot \exp\left(\frac{-\Delta F}{R.T}\right) \quad (2)$$

where the first exponential corresponds to the molecular diffusion describing the transport which takes place when molecular segments are added to the crystal. The second exponential describes the process of nucleation. Both terms show an opposite behavior and that is why the curve presents a maximum. From the equation of Turnbull is obtained the Lauitzen and Hoffmann equation as follow:

$$G = G_o \cdot \exp\left(\frac{-U}{R(T - T_{\infty})}\right) \cdot \exp\left(\frac{-K_G}{fT\Delta T}\right) \quad (3)$$

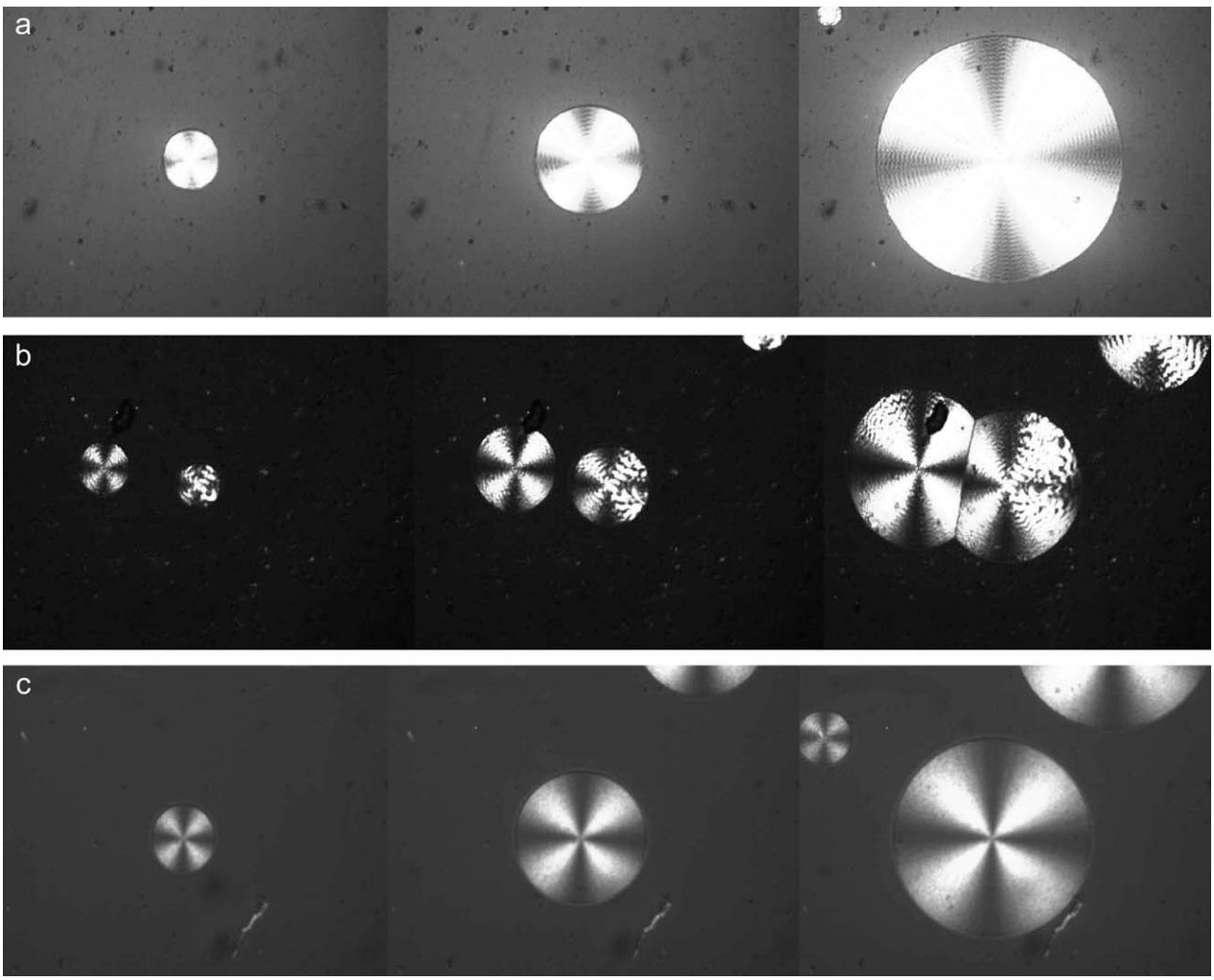

Figure 7 Micrograph obtained by POM. Temperature of crystallization = 90°C. 100X to: (a) PHB, (b) PHB/4%CNa^+, and (c) PHB/4%C15A.

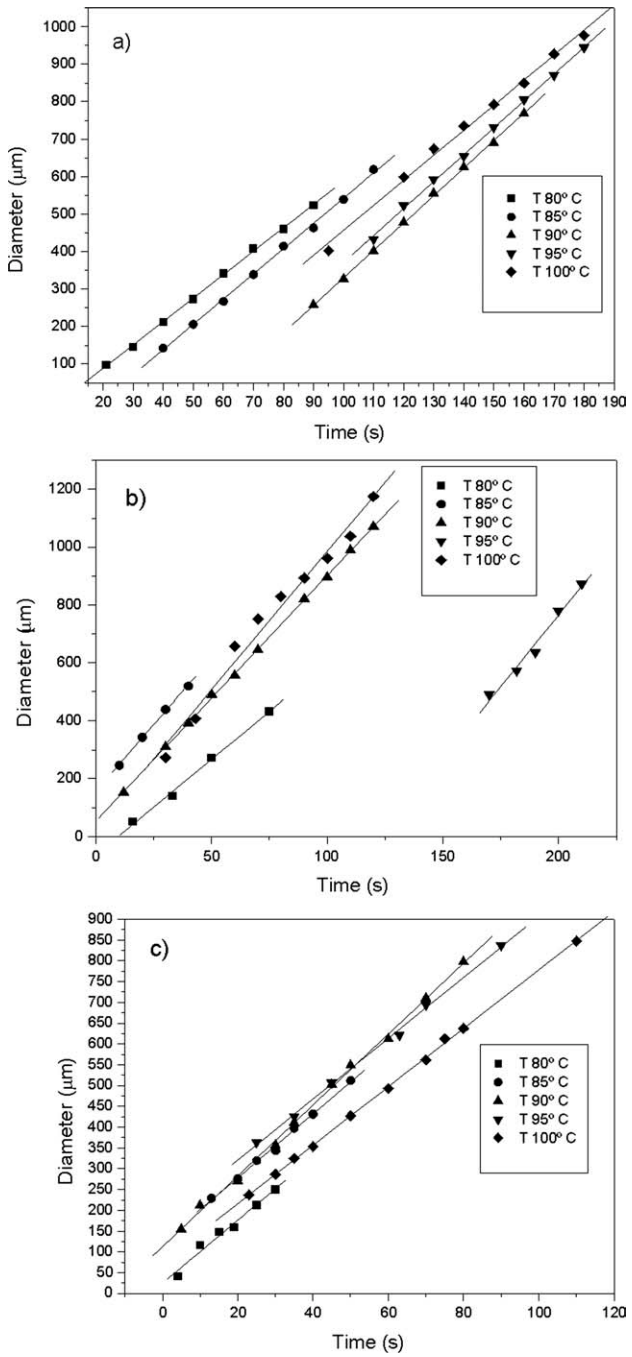

Figure 8 Time evolution of the diameter of spherulites of: (a) PHB, (b) PHB/4%CNa^+, and (c) PHB/4%C15A for isothermal crystallization at the indicated temperatures.

where *Go* is a constant which is temperature independent, *U* is the activation energy for the transport of the crystallizable segments, T_∞ is an hypothetical temperature to which the molecular motion associated with the viscous flow stops and it is related to T_g by $T_\infty = T_g$ - *C* where *C* is a constant; ΔT: is the degree of supercooling, given by $T_m - T_c$; T_m is the equilibrium melting point; *f* is a factor which represents the variation of the enthalpy in the bulk per

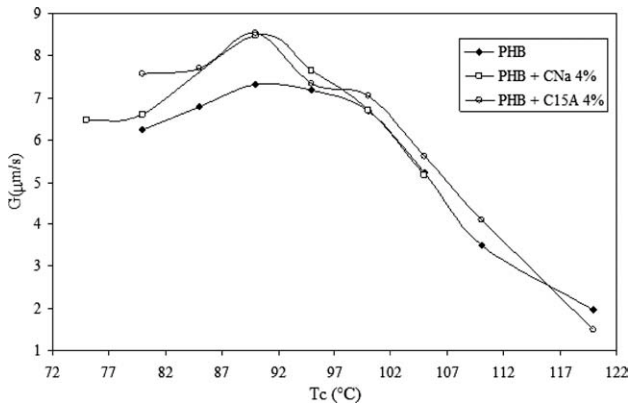

Figure 9 Radial growth rate (*G*) as a function of crystallization temperature for PHB, PHB/4%CNa^+, and PHB/4%C15A.

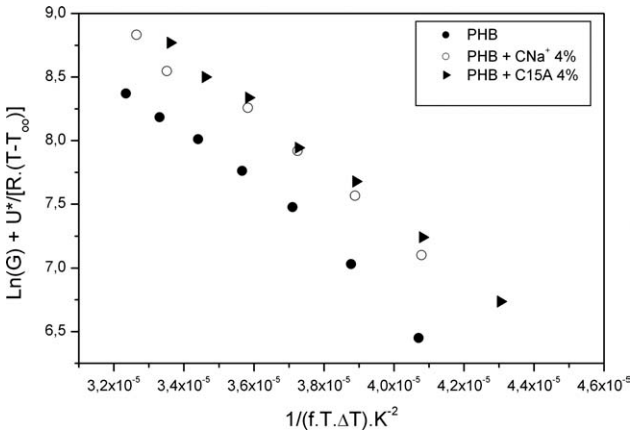

Figure 10 Plots of $\mathrm{Ln}(G) + U/[R.(T - T_\infty)]$ versus $1/(f.T.\Delta T)$ for PHB and their nanocomposites.

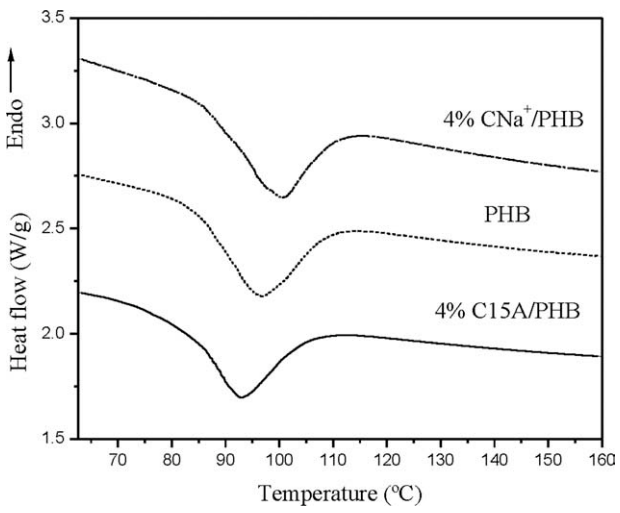

Figure 11 DSC thermogram of PHB and their nanocomposites with 4% of clay at 5°C/min cooling rate.

TABLE IV
Parameters Obtained to the Nonisothermal Crystallization Exotherm Peak

Material	T_p °C	T_i °C	T_f °C	t_c (min)	ΔW
PHB	97	116	78	7.7	15
PHB + 4% CNa^+	100	116	76	8.0	14
PHB + 4% C15A	93	110	72	7.7	14

unit volume with the temperature, given by $f = \frac{2T}{Tm+T}$; K_G is the nucleation constant.[29]

Then, applying *ln* in both members of the eq. (3), the following linearized expression is obtained:

$$\ln(G) + \frac{U}{R(T - T_{oo})} = ln(G_o) - \frac{K_G}{fT\Delta T} \quad (4)$$

According to this equation, a straight line from the plot of $lnG + U/R(T - T_\infty)$ versus $1/fT\Delta T$ should be obtained. However, as it is necessary to know the value of U and T_∞, the universal value found by Suzuki-Kovacs: $U = 1500$ cal mol^{-1}, $C = 30$ K, was used to do the adjustment of the experimental data. A very good fit to the experimental data was obtained (Fig. 10) and the K_G values were calculated from the slopes. The nucleation constant values are lesser in the nanocomposites (PHB + 4% CNa^+: $2.04 \times 10^5\ k^2$; PHB + 4% C15A: $2.12 \times 10^5\ k^2$) than in the PHB ($2.25 \times 10^5\ k^2$). These results showed that clays do not accelerate the formation of PHB spherulites nucleus.

The variation in the parameters from nonisothermal crystallization curves, from the melted samples indicates differences in the crystallization behavior, comparing the polymer and their nanocomposites.[7] Figure 11 compares the heat flow development during cooling at 5°C/min for PHB and PHB/clay nanocomposites. The crystallization parameters obtained from the DSC curves (Table IV) are the onset crystallization temperature (T_i), end crystallization temperature (T_f), peak temperature of the crystallization exotherm (T_p), the crystallization time $t_c = T_i - T_f/v$, where v is the velocity of the scan, and the width at half-height of the exotherm peak (ΔW). The peak width at half-height, ΔW, is a measure of the crystallite size distribution. No appreciable differences in the parameters obtained from the nonisothermal crystallization peak were observed. These data confirms that the clays affect a little the nucleating behavior of PHB, in accordance with the POM results.

It was observed that the maximum in the degradation temperature with the percentage of clay is in accordance with the maximum in the percentage of crystallinity. Then, the crystallinity is another factor, which affects the thermal degradation behavior.

CONCLUSIONS

A series of nanocomposites of PHB with nonmodified (CNa^+) and organically modified (C15A) MMTs were prepared by casting, from a homogeneous dispersion of clay and PHB.

The nanocomposites studied showed a different thermal degradation behavior. The addition of Cloisite® 15A enhanced the thermal resistance of PHB while the addition of Cloisite® Na^+ decreased it. It could be explained due to the presence of two opposite effects: the physical barrier, chain mobility, and the catalytic activity of the clay.

The more hydrophobic clay (C15A) was the best dispersed in the PHB in spite of the expansion of the CNa^+ layers. It could be due to the higher initial interlayer gallery of the C15A as well as the better compatibility between the clay and the polymer.

The clay produced a slight diminution in the percentage of PHB crystallinity, but the overall morphology did not change. However, it was observed that the addition of clay enhanced the crystallization rate of PHB, but it would not act as a nucleating agent.

The slightly increment in the Young's modulus of the nanocomposite containing C15A was related to the better dispersion of the clay in the polymer matrix.

References

1. Van der Walle, G. A. M.; Buisman, G. J. H.; Weusthuis, R. A.; Eggink, G. Int J Biol Macromol 1999, 25, 123.
2. Xu, J.; Guo, B.; Rui Yang, R.; Wub, Q.; Guo-Qiang Chen, G.; Zhang, Z. Polymer 2002, 43, 6893.
3. Sudesh, K.; Abe, H.; Doi, Y. Prog Polym Sci 2000, 25, 1503.
4. Bordes, P.; Hablot, E.; Pollet, E.; Avérous L. Polym Degrad Stab 2009, 94, 789.
5. Avella, M.; Maruscelli, E.; Raimo, M. Polymer 1993, 34, 3234.
6. Bordes, P.; Pollet, E.; Avérous, L. Prog Polym Sci 2009, 34, 125.
7. Botana, A.; Mollo, M.; Eisenberg, P.; Torres Sanchez, R. Appl Clay Sci 2010, 47, 263.
8. Cyras, V. P.; Vázquez, A.; Rozsa, Ch.; Galego Fernandez, N.; Torre, L.; Kenny, J. M. J Appl Polym Sci 2000, 77, 2889.
9. Huang, M.-F.; Yu, J.-G.; Ma, X.-F.; Jin, P. Polymer 2005, 46, 3157.
10. Pukánszky, B.; Müller, P.; Bagdi, K. Compos Interfaces 2006, 13, 1.
11. Cyras, V. P.; Manfredi, L. B.; Ton-That, M.-T.; Vázquez, A. Carbohydr Polym 2008, 73, 55.
12. Ray, S. S.; Okamoto, M. Prog Polym Sci 2003, 28, 1539.
13. Aboulkas, A.; El Harfi, K.; El Bouadili, A. Energy Convers Manage 2008, 49, 3666.
14. Cyras, V. P.; Galego Fernandez, N.; Vázquez, A. Polym Int 1999, 48, 705.
15. Chiu, H.-J. Polymer 2005, 46, 3906.
16. Zhao, C.; Qin, H.; Gong, F.; Feng, M.; Zhang, S.; Yang, M. Polym Degrad Stabil 2005, 87, 183.
17. Davis, R. D.; Gilman, J. W.; Vander Hart, D. L. Polym Degrad Stabil 2003, 79, 111.

18. Maiti, P.; Batt, C. A.; Giannelis, E. P. Polym Mater Sci Eng 2003, 88, 58.
19. Duquesne, S.; Jama, C.; Le Bras, M.; Delobel, R.; Recourt, P.; Gloaguen, J. M. Compos Sci Technol 2003, 63, 1141.
20. Beyer, G. Plast Addit Compound 2002, 4, 22.
21. Lim, S. T.; Hyun, Y. H.; Lee, C. H.; Choi, H. J. J Mater Sci Lett 2003, 22, 299.
22. Cerruti, P.; Ambrogi, V.; Postiglione, A.; Rychly, J.; Matisova-Rychla, L.; Carfagna, C. Biomacromolecules 2008, 9, 3004.
23. Rohlmann, C.; Horst, M. F.; Quinzani, L.; Failla, M. Eur Polym Mater 2008, 44, 2749.
24. Paul, D. R.; Robeson, L. M. Polymer 2008, 49, 3187.
25. Bordes, P.; Pollet, E.; Bourbigot, S.; Averous, L. Macromol Chem Phys 2008, 209, 1473.
26. Lim, S. T.; Hyun, Y. H.; Choi, H. J Chem Mater 2002, 14, 1839.
27. Turnbull, D.; Fisher, J. C. J Chem Phys 1949, 17, 71.
28. Peng, S.; An, Y.; Chen, C.; Fei, B.; Zhuang, Y.; Dong, Y. Eur Polym Mater 2003, 39, 1475.
29. Hoffman, J. D. Polymer 1983, 24, 3.